Acta Neuropathol (1997) 93 : 354–368

REGULAR PAPER

Akihiro Takahashi · Hun K. Park · Miguel A. Melgar
Luis Alcocer · Jaime Pinto · Tiffanee Lenzi
Fernando G. Diaz · José A. Rafols

Cerebral cortex blood flow and vascular smooth muscle contractility in a rat model of ischemia: a correlative laser Doppler flowmetric and scanning electron microscopic study

Received: 2 July 1996 / Revised, accepted: 24 September 1996

Abstract The present study was undertaken to ascertain the role of smooth muscles and pericytes in the microcirculation during hyperperfusion and hypoperfusion following ischemia in rats. Paired external carotids, the pterygopalatine branch of the internal carotids and the basilar artery were exposed and divided. Reversible inflatable occluders were placed around the common carotids. After 24 h, the unanesthetized rat underwent 10-min ischemia by inflating the occluders. Continuous cortical cerebral blood flow (c-CBF) was monitored by laser Doppler flowmetry. The measured c-CBF was below 20% of control ($P < 0.001$) during ischemia. A c-CBF of 227.5 ± 54.1% ($P < 0.001$) was obtained during reperfusion hyperemia. A c-CBF of 59.7 ± 8.8% ($P < 0.001$) occurred at the nadir of postischemic hypoperfusion, and this was followed by a second hyperemia. The cytoarchitecture of the vascular smooth muscles and pericytes was assessed by scanning electron microscopy. Samples were prepared using a KOH-collagenase digestion method. In control rats, arteriolar muscle cells showed smooth surfaces. Capillary pericytes were closely apposed to the endothelium. Immediately after reperfusion, transverse membrane creases were observed on the smooth muscle surfaces. During maximal hyperemia the creases disappeared. When c-CBF started to decrease the creases became visible again. Throughout the postischemic hypoperfusion the creases remained. Capillary endothelial walls became tortuous in the late phase of hypoperfusion. During the second hyperemia most arteriolar muscle cells showed smooth surfaces. Some pericytes appeared to have migrated from the vascular wall. The morphological changes of smooth muscle membranes suggest that they are related to specific perfusional disturbances during ischemia and reperfusion.

Key words Reperfusion · Cerebral blood flow · Vascular smooth muscle cell · Pericyte · Scanning electron microscopy

A. Takahashi · H. K. Park · M. A. Melgar · L. Alcocer · J. Pinto
F. G. Diaz
Department of Neurosurgery,
Wayne State University School Medicine,
University Health Center, 4201 St. Antoine 6E,
Detroit, MI 48201, USA
Tel.: 1-313-745-4661; Fax: 1-313-745-4099

T. Lenzi · J. A. Rafols (✉)
Department of Anatomy and Cell Biology,
Wayne State University School of Medicine, 540 E. Canfield,
Detroit, MI 48201, USA
Tel.: 1-313-577-41049; Fax: 1-313-577-3125;
e-mail: jrafols@med.wayne.edu

Introduction

Transient interruption of cerebral blood flow (CBF) and reperfusion is a common event in the surgical treatment of complex aneurysms [7, 29] and carotid artery stenosis [30], as well as after thrombolytic therapy for embolic stroke [10, 80]. Although reperfusion of ischemic tissue may be thought to contribute to its recovery, extensive clinical and experimental studies [6, 13, 22, 78] have shown that untimely reperfusion results in irreversible tissue injury which cannot be attributed to the ischemic insult alone.

Transient global or focal ischemia in many animal species [16, 17, 36, 38, 44, 47, 56, 60, 64, 67, 72, 73] is followed initially by a brief period of hyperperfusion (reperfusion hyperemia) and, subsequently, by a below normal perfusion (postischemic hypoperfusion). The reperfusion hyperemia has been associated with the opening of blood-brain barrier (BBB) and vasogenic edema [9, 37, 60, 67] where extravasated plasma constituents could compromise neuronal survival [30]. Concurrent with hyperemia is the excess delivery of O_2 to the tissue which is biochemically set to release a burst of arachidonic acid metabolites [11] and oxygen free radicals [28, 74]. These molecular events are coupled with the restitution of glucose to ischemic tissues, leading to sustained lactoacidosis because of continued formation of lactate [1]. In summary, hyperemia has been envisioned by some investigators [50, 56, 68] as an onrush of blood flow through ves-

sels maximally dilated by lactoacidosis and devoid of autoregulation by the previous ischemic insult.

In contrast, increases in both oxygen extraction and metabolism, suggesting an uncoupling between metabolic demand and substrate delivery, have been reported during postischemic hypoperfusion [12, 27, 36, 38, 64, 67]. Different explanations for the decreased CBF have been proposed including: (1) rheological changes, microvascular obstruction due to the aggregation of blood elements [23, 51] and hemoconcentration, (2) capillary obstruction by endothelial microvilli formation [14], (3) compression of vascular lumen by cellular (neurons, glia, and endothelium) and/or extracellular swelling [50, 53], and (4) increased vascular smooth muscle tone. Of these, the last explanation has been least documented. Although many studies [17, 40, 47, 56, 68, 72] have suggested that an increased smooth muscle tone of the microcirculation contributes significantly to postischemic perfusion disturbances, little is known as to how the ischemic stroke affects the smooth muscle tone [24]. Some investigators [44, 68] observed directly serial changes in the diameter of pial arterioles with diameters of over 50 μm through an artificially made cranial window. However, this method did not allow visualization of the parenchymal microvessels which may be involved in reperfusional injury [15].

Two other factors are important in determining the role of the vascular smooth muscle in postischemic microcirculation, one is the reliability of the forebrain ischemia model used, and the other is the methodology employed to accurately measure CBF. To the best of our knowledge, the most reliable forebrain ischemia model without systemic effects is the rat seven vessel occlusion (7VO) model described by Shirane et al. [63]. This model, however, produced a high mortality rate due to respiratory complications. Recently we have modified and extended this model with substantial improvement of the mortality rate [45]. In addition we have used a new method for measuring cortical CBF (c-CBF) in awake rats by applying laser Doppler flowmetry (LDF) as described previously by Sato et al. [61]. This method allows us to measure c-CBF changes accurately and on-line in unanesthetized animals by tightly attaching the LDF probe to a specific region of the brain through a guiding cannula.

Using these improved methods we undertook the study of the morphological changes of the smooth muscle in rat cerebral cortex microcirculation during global ischemia and reperfusion. We have correlated the temporal profile of the c-CBF with the changes in smooth muscle contractility in the wall of microvessels observed under the scanning electron microscope (SEM). This study uses a KOH-collagenase partial digestion method [69–71, 76, 77] for observing the outer surfaces of smooth muscles without affecting their fine structure. The present data add new insights into the role of the parenchymal vascular smooth muscle and how it may be related to temporally defined c-CBF changes during ischemia and reperfusion.

Materials and methods

All animal experiments were approved by our institutional review board and were conducted in compliance with the "Principles of Laboratory Animal Care" (NIH publication no. 86–23, revised 1985).

Surgical preparation

Male Sprague Dawley rats (n = 44) weighing 375–400 g were housed under diurnal lighting condition and given free access to food and water before the experiments. The rats were pretreated with an intramuscular injection of atropine sulfate (1 mg/kg) and anesthetized with an intraperitoneal injection of chloral hydrate in normal saline (400 mg/kg). Additional aliquots of chloral hydrate were administered when required. The animals were orotrachially intubated with a 16-gauge angiocatheter, and mechanically ventilated (small animal ventilator, Harvard Instrument, Cambridge, Mass.) with room air.

Vessel occlusion

The rat model of 7VO has been described in detail [45, 63]. Briefly, each rat was fixed in the supine position. Through a midline neck incision, paired external carotid arteries and the pterygopalatine branch of the internal carotid arteries were exposed, electrically cauterized and divided. The trachea and the esophagus were retracted gently to a medial side and part of the longus capitis was cauterized and removed, not only to expose the ventral surface of the clivus, but also to reduce the degree of retraction of the trachea and the esophagus. A small hole was drilled at the midportion of the clivus exposing the brain stem. The dura mater and the arachnoid membrane were opened, and the basilar artery was cauterized and divided. The bony defect was then filled with Gelfoam (Upjohn, Kalamazoo, Mich.). Both common carotid arteries were exposed and isolated from the carotid sheaths taking care not to damage the vagus nerves. Reversible inflatable balloon occluders (OC2A, In Vivo Metrics, Healdsburg, Calif.) were placed around the common carotid arteries, with the distal ends of the occluders externalized through holes at the rat's back and secured to the skin.

Hematological measurement

Following vessel occlusion, a PE-50 polyethylene catheter filled up with heparinized saline (100 IU heparin in 1 ml saline) was inserted into the caudal artery and secured. Cotton, containing 1% procaine hydrochloride, was placed in the wound area. After regaining consciousness, the rats were placed at an ambient temperature and allowed free access to water. After 24 h, the unanesthetized animal underwent 10 min of ischemia by inflating both occluders simultaneously with syringes. Blood samples were collected from the arterial tail catheter at the following times: (1) before ischemia, (2) midtime during ischemia, (3) 5 min after recirculation, and (4) 60 min after recirculation. Blood gases, pH, hematocrit, and blood glucose level (Stat profile 5, Nova Biomedical, Waltham, Mass.) were measured in a group of six rats.

Measurement of c-CBF

A separate group of seven rats was used for the CBF studies. Following vessel surgery and arterial catheter insertion, each rat was placed in the prone position. Through a midline scalp incision of about 3 cm in length, a burr hole (3×3 mm^2) was drilled over the right frontoparietal sensorimotor cortex at stereotaxic coordinates +0.5 to –2.5 mm anteroposterior, and +1.5 to +4.5 mm right from the bregma, according to Paxinos and Watson [52]. Special attention was taken not to damage the dura mater. A modification of the

LDF method for continuous measurement of c-CBF in the conscious rat as described by Sato et al. [61] was used. An acrylic plate of about 10x6 mm^2 area, and 1 mm thick provided with two holes at both edges was placed over the hole in the skull. Two small screws (bone anchor type; Stoeling, Wood Park, Ill.) were used to fix the acrylic plate to the skull. On this acrylic plate, a guiding cannula (outer diameter 1.52 mm, inner diameter 0.76 mm and length 9.5 mm, PE-100, Becton Dickinson, Sparks, Md.) for the LDF probe was positioned perpendicularly above the cortical surface, avoiding visible blood vessels. Both the plate and cannula were fixed to each other with dental cement (Fig. 1A). After regaining consciousness, rats were housed at an ambient temperature, and allowed free access to water. After 23 h, each rat was anesthetized with 3% halothane for 2–3 min. Immediately after anesthesia, the rat was placed in a handmade hammock suspended from a plastic frame (Fig. 1B) to achieve partial restraining during the gathering of data. An LDF probe (P-433-1; Vasomedic, St. Paul, Minn.), with outer diameter 0.8 mm and length 10 mm, for LDF (Laserflo BPM^2, Vasomedics) was then inserted into the cannula and the c-CBF value was continuously displayed on a monitor. Concurrently, the end of an arterial catheter was connected to a pressure transducer (Transpac II; Abbott Laboratories, North Chicago, Ill.) and mean arterial blood pressure (MBP) was displayed on a blood pressure monitor (78342A; Hewlett Packard, Boeblingen, Germany). Both c-CBF and MBP values were A/D converted (DT21-EZ, Data Translation, Malboro, Mass.) and processed on a personal computer using an appropriate software (Labtech Notebook; Laboratory Technology, Wilmington, Mass.).

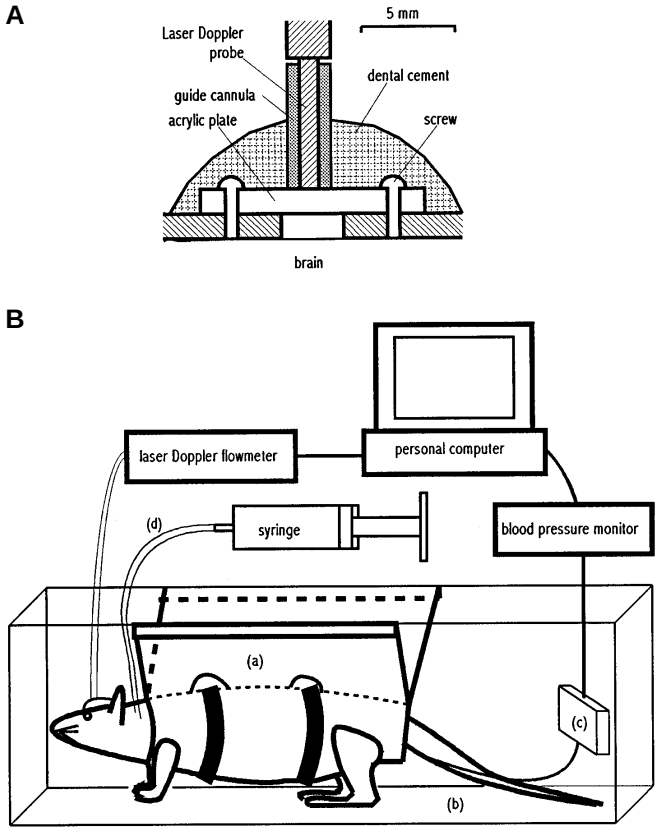

Fig. 1A, **B** Diagrams of the experimental protocol used in this study. **A** Fixation of the laser Doppler flowmeter probe in the guiding cannula on the skull. **B** The unanesthetized rat placed in a hand-made hammock (*a*) and suspended from a plastic box (*b*) for recording of cortical cerebral blood flow and systemic blood flow. (*c* pressure transducer, *d* the distal end of the inflatable balloon occluder)

Recording of physiological variables began 1 h after halothane anesthesia. Baseline c-CBF value in each rat was established by averaging values (n = 7) measured during the 5 min before ischemia. Initially, control values of c-CBF and MBP were measured every 10 s for 5 min. Subsequently, the same physiological parameters were measured every 10 s for 40 min throughout 10 min of forebrain ischemia and 30 min of reperfusion. After the reperfusion period, the same parameters were measured every 5 min for 24 h. All experiments were performed under constant lighting conditions.

Statistical analysis

All data were expressed as mean ± SD of the indicated number of rats. The significance of statistical analysis was determined by the Student's t-test. Only values of $P < 0.05$ were accepted as statistically significant.

Preparation of tissues for SEM

Experimental animals were grouped on the basis of the c-CBF changes: immediately after reperfusion, at 8, 15, 30, and 90 min, and 6, 12, and 24 h after reperfusion (n = 4 for each time point). Animals in each time group were anesthetized with chloral hydrate and perfused transcardially (head pressure equivalent to 150 cm H_20) with 0.1 M phosphate buffer (PB) (pH 7.4) followed by a fixative containing 2.0% paraformaldehyde and 2.5% glutaraldehyde in 0.1 M PB (pH 7.4). Tissues were also obtained from normal (n = 2) and sham-operated (n = 2) controls. The latter group consisted of animals treated surgically like the experimental groups but without ischemia and reperfusion. The head pressure used to perfuse the brains of the normal and sham-operated controls was identical to that used for the experimental brains. Following removal, brains were immersed in the same fixative at room temperature for 1 day. The fixed brain was then cut into a block, of approximately 5 × 5 mm^2 area by 2 mm in depth, which contained the sensorimotor cortex from the center of which the c-CBF measurement had been determined.

To observe the adventitial surface of smooth muscles, the collagenous tissue of the fixed specimens was removed using a KOH-collagenase digestion method [69–71, 76, 77]. Briefly, the specimens were placed in 30% KOH at 65°C for about 10 min and then immersed in a 0.1% collagenase (Sigma, type II) in 0.1 M PB (pH 7.4) at 37°C for 5 h. The digested specimens were conductive stained by a tannin-osmium method [49], dehydrated in a graded series of ethanol and critical-point dried with liquid CO_2. The dried specimens were mounted on aluminum stubs, coated with platinum in an ion coater, and observed with a SEM (JSM-840A, JEOL, Tokyo, Japan) at 25 kV. Analyses of intraparenchymal vessels were restricted to terminal and precapillary arterioles and capillaries (n = 20 for each type of vessel). Intraparenchymal veins were not analyzed because the integrity of their wall was often compromised in the process of tissue puncturing and separation prior to SEM study.

Results

Behavioral changes

Loss of the righting reflex and decerebrate rigidity occurred immediately after inflating the balloon occluders. Spontaneous respiration was maintained during ischemia and reperfusion, reflecting adequate irrigation of the vital centers of the brain stem. All rats regained the righting reflex within 1 h after deflating the occluders. However, ambulatory movements were slow, and general alertness was diminished for the duration of the experiments.

Loosely restrained rats remained calm during the gathering of blood flow data.

Physiological variables

Measurements of arterial blood gases and glucose levels in control and experimental rats remained within normal ranges (Table 1). The LDF accurately reflected relative changes in c-CBF, but absolute values were dependent on probe placement. c-CBF changes were expressed as a percentage of the preischemic baseline value for c-CBF set at 100%. Figure 2 shows a composite graph of the c-CBF (n = 7) measured for 24 h. In all animals the c-CBF dropped below 20% of baseline values within 20 s after inflating the balloon occluders. It remained close to this value (mean of 18.9 ± 13.3%, $P < 0.001$) at midpoint (after 5 min) and throughout the remainder of the ischemic period. After deflating the occluders, c-CBF values increased rapidly, returning to baseline within 2 min after reperfusion. The maximum hyperemic c-CBF mean value of 227.5 ± 54.1% ($P < 0.001$) occurred after 8 min of reperfusion. Subsequently, hyperemia c-CBF values fluctuated for 7 min with a mean value of 214.0 ± 79.2% ($P < 0.05$), after which they decreased precipitously. The c-CBF returned to baseline values after approximately 27 min of reperfusion. The mean duration of the first hyperemia was estimated at 25 ± 2 min (reperfusion hyperemia). Subsequently the c-CBF continued decreasing below baseline values reaching its nadir at a mean of 59.7 ± 8.8%, ($P < 0.001$) at 90 min of reperfusion. After fluctuating below baseline values, c-CBF returned to baseline values by 8 h and 30 min of reperfusion. Therefore, the duration of the postischemic hypoperfusion lasted approximately 8 h. After this delayed hypoperfusion the c-CBF fluctuated above the baseline value (second hyperemia) for 15 h until the end of the experiment. A mean c-CBF value of 122.8 ± 83.9% was obtained at 12 h of reperfusion. This last value was not statistically significant due to a large standard deviation.

Table 1 Physiological variables in the rat before, during, and following seven-vessel occlusion (n = 6)

	Control	During ischemia	5 min after reperfusion	60 min after reperfusion
pH	7.44 ± 0.06	7.41 ± 0.09	7.45 ± 0.09	7.45 ± 0.09
PaO2	93.28 ± 9.19	91.03 ± 13.53	88.64 ± 10.00	99.05 ± 11.74
PaCO2	30.86 ± 3.58	33.85 ± 10.64	32.65 ± 9.56	32.67 ± 9.48
Glucose	142 ± 37	166 ± 14	186 ± 30	181 ± 26
Hematocrit	51.83 ± 8.82	45.00 ± 5.96	49.17 ± 5.49	53.67 ± 6.12

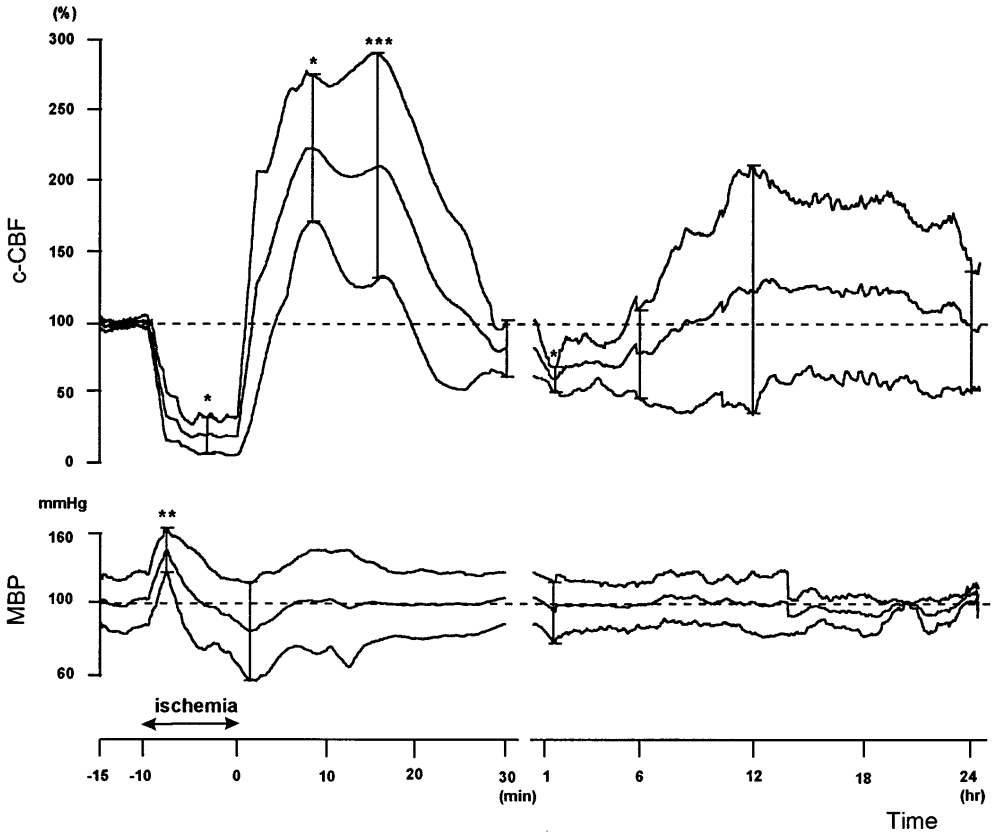

Fig. 2 Cortical cerebral blood flow (*c-CBF*) and mean arterial blood pressure (*MBP*) changes in seven rats. c-CBF was assessed by laser Doppler flowmeter on the right sensorimotor cortex with values expressed as a percentage of baseline values. *$P < 0.001$, **$P < 0.01$, ***$P < 0.05$ significantly different from the baseline values

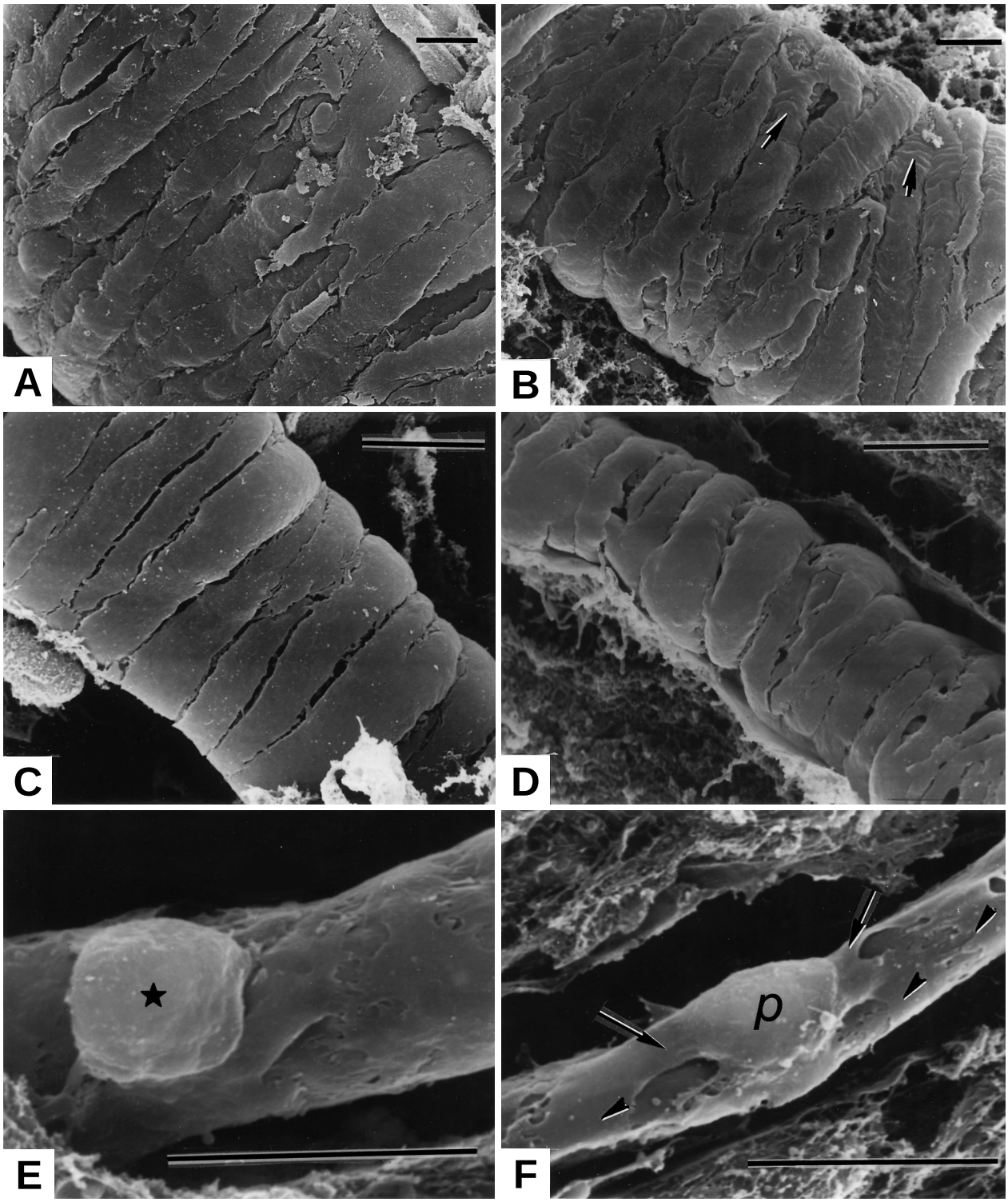

Fig. 3A–F Scanning electron micrographs of control rats. **A** A muscular arteriole measuring about 80 µm in diameter on the brain surface. The tunica media consists of two to three layers of muscle cells with smooth surfaces. **B** A muscular arteriole measuring about 60 µm in diameter on the brain surface. Ripple-like undulations (*arrows*) are seen on the smooth muscle surfaces. **C** A terminal arteriole measuring about 25 µm in diameter on the brain surface. The tunica media consists of a monolayer of muscle cells with smooth surfaces. **D** A terminal arteriole measuring 17 µm in the brain parenchyma with smooth cell surfaces. **E** A precapillary arteriole measuring 8 µm in diameter found in the brain parenchyma. A smooth muscle cell has a characteristically bulging cell body (*star*) with thick processes which wind helically around the endothelium. **F** A capillary about 5 µm in diameter found in the brain parenchyma. The pericyte surmounting this capillary possesses an ovoid cell body (*p*) which extends two longitudinal primary processes (*arrows*) along the vessel. These processes give rise to secondary processes (*arrowheads*) which tightly surround the endothelial tube. *Bars* = 10 µm

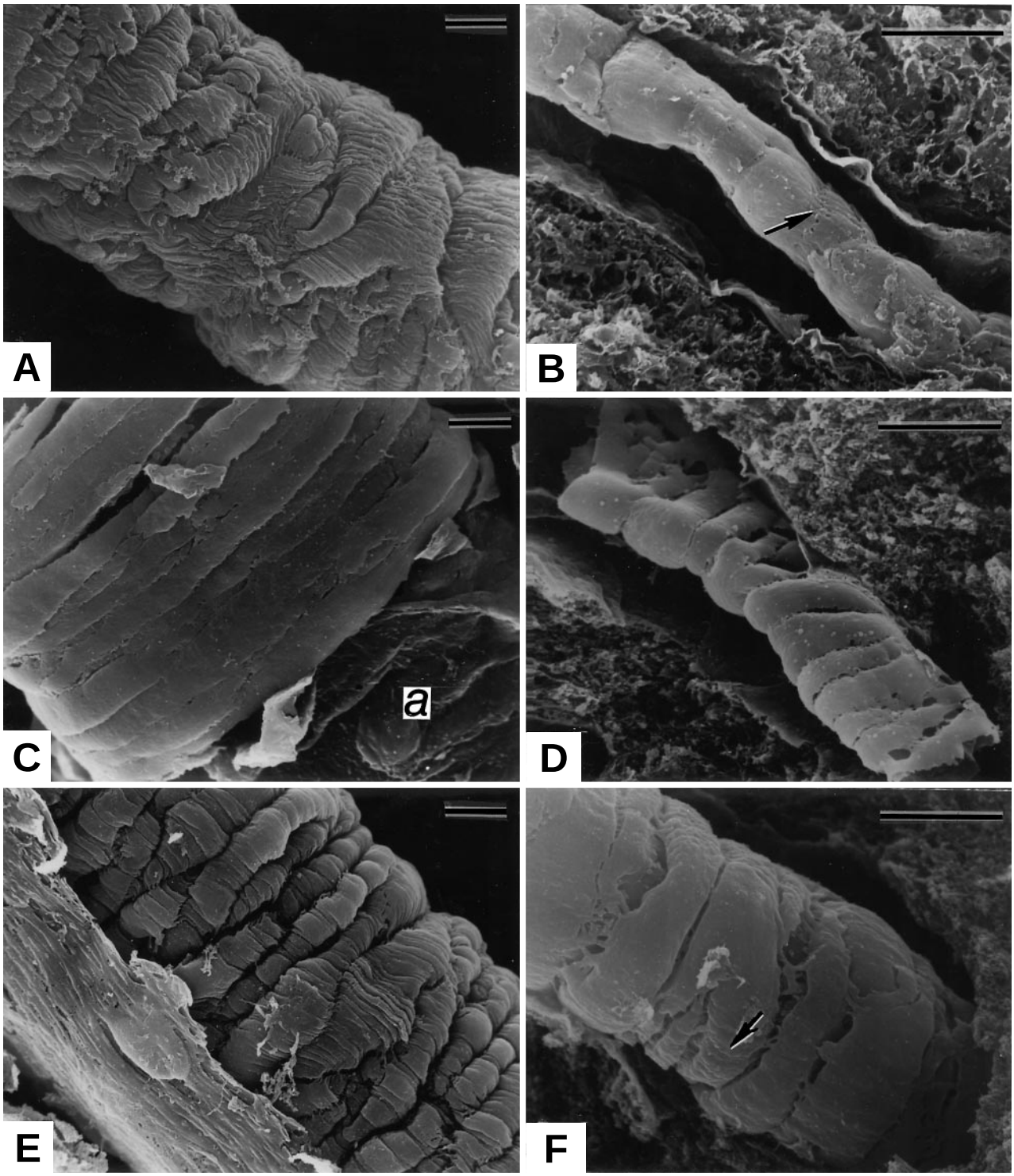

Fig. 4 Micrographs showing temporal changes of muscular arterioles on the brain surface (**A**, **C**, **E**) and terminal arterioles in the brain parenchyma (**B**, **D**, **F**) immediately after reperfusion (**A**, **B**), at 8 min of reperfusion (**C**, **D**) and at 15 min of reperfusion (**E**, **F**). **A** Transverse or oblique folds are prominent on the smooth muscle surfaces. **B** Shallow undulations (*arrow*) are seen on the smooth muscle surfaces. **C**, **D** Muscle cells with smooth surfaces. Transverse folds (**E**) or undulations (*arrow*, **F**) are seen on the muscle cells. *Bars* = 10 μm

In contrast, baseline MBP values averaged 102 ± 15 mm Hg. MBP mean values increased immediately (within 2.2 min) after inflating the occluders (133 ± 13 mm Hg, $P < 0.01$). After this initial rise, MBP values returned to baseline values within 5 min and then decreased below normal values (85 ± 29 mm Hg, non-significant) after 1.6 min of reperfusion. After this decline MBP returned to baseline values by 6.8 min of reperfusion. The data of the two concurrent measurements therefore indicate that the

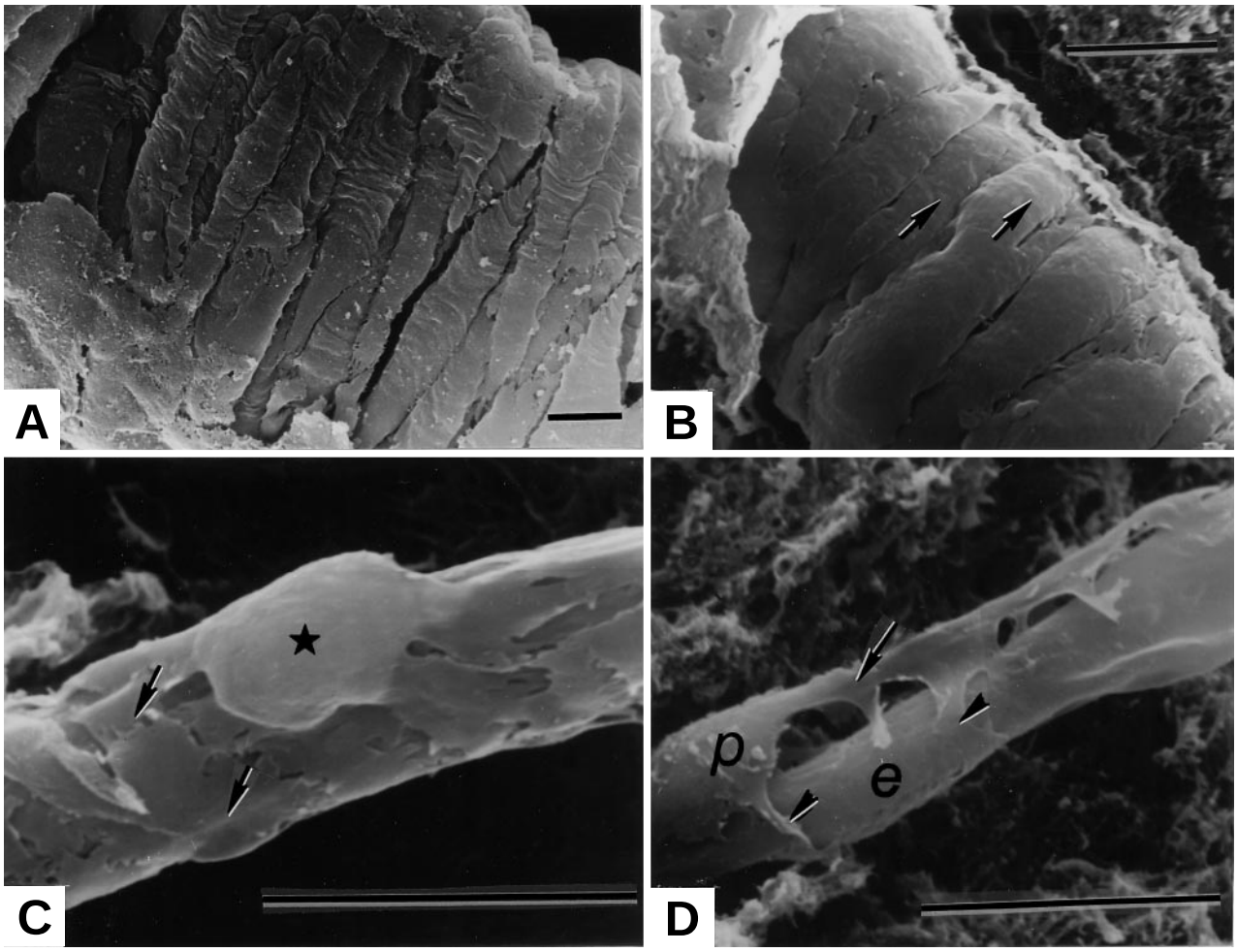

Fig. 5A–D Micrographs at 90 min of reperfusion. **A** A muscular arteriole on the brain surface. Transverse or oblique folds remains on the smooth muscle surfaces. **B** A terminal arteriole found in the brain parenchyma with membrane undulations (*arrows*). **C** A precapillary arteriole found in the brain parenchyma. A smooth muscle cell with a bulging cell body (*star*) from which processes with scalloped contours (*arrows*) originate. **D** A capillary in the brain parenchyma. The cell body (*p*) and primary process (*arrow*) of this pericyte appear detached from the endothelial tube (*e*). Secondary processes (*arrowheads*) retain partial apposition with the endothelial tube. *Bars* = 10 μm

reperfusion hyperemia was independent of MBP. Although MBP values decreased slightly to 97 ± 18 mm Hg, in relation to the hypoperfusion nadir, this was not statistically significant. Similarly, the remaining postischemic hypoperfusion and second hyperemia appeared, likewise, to be independent of MBP.

SEM observations

Based on previously established morphological criteria pertinent to vessels of different sizes [62, 77], observations were made on: (1) muscular arterioles, (2) terminal arterioles, (3) precapillary arterioles, and (4) capillaries.

Normal and sham-operated controls

Smooth muscles of the muscular and terminal arterioles on the brain surface were observed under the SEM at regions where arachnoid cells and adventitial elastic tissues had been peeled off by KOH-collagenase digestion.

Muscular arterioles, measuring 30–100 μm in diameter, were found primarily on the brain surface. The wall of these arterioles typically consisted of two or three layers of circularly arranged smooth muscle cells. The smooth muscle cells were usually spindle-shaped with smooth surfaces (Fig. 3A). A few ripple-like undulations, disposed perpendicularly to the long axis of the muscle cell, were found occasionally on the adventitial surface in normal specimens (Fig. 3B). These undulations, however, were rarely observed in the sham-operated control specimens. Furthermore, terminal arterioles, measuring 10–30 μm, had a wall consisting of a monolayer of spindle-shaped smooth muscle cells with smooth surfaces (Fig. 3C).

By puncturing and separating the specimen with a fine needle, blood vessels within the brain parenchyma became accessible for observation under the microscope. Analyses of parenchymal terminal arterioles, precapillary arterioles, and capillaries were then undertaken. In general the cytoarchitecture of terminal arterioles within

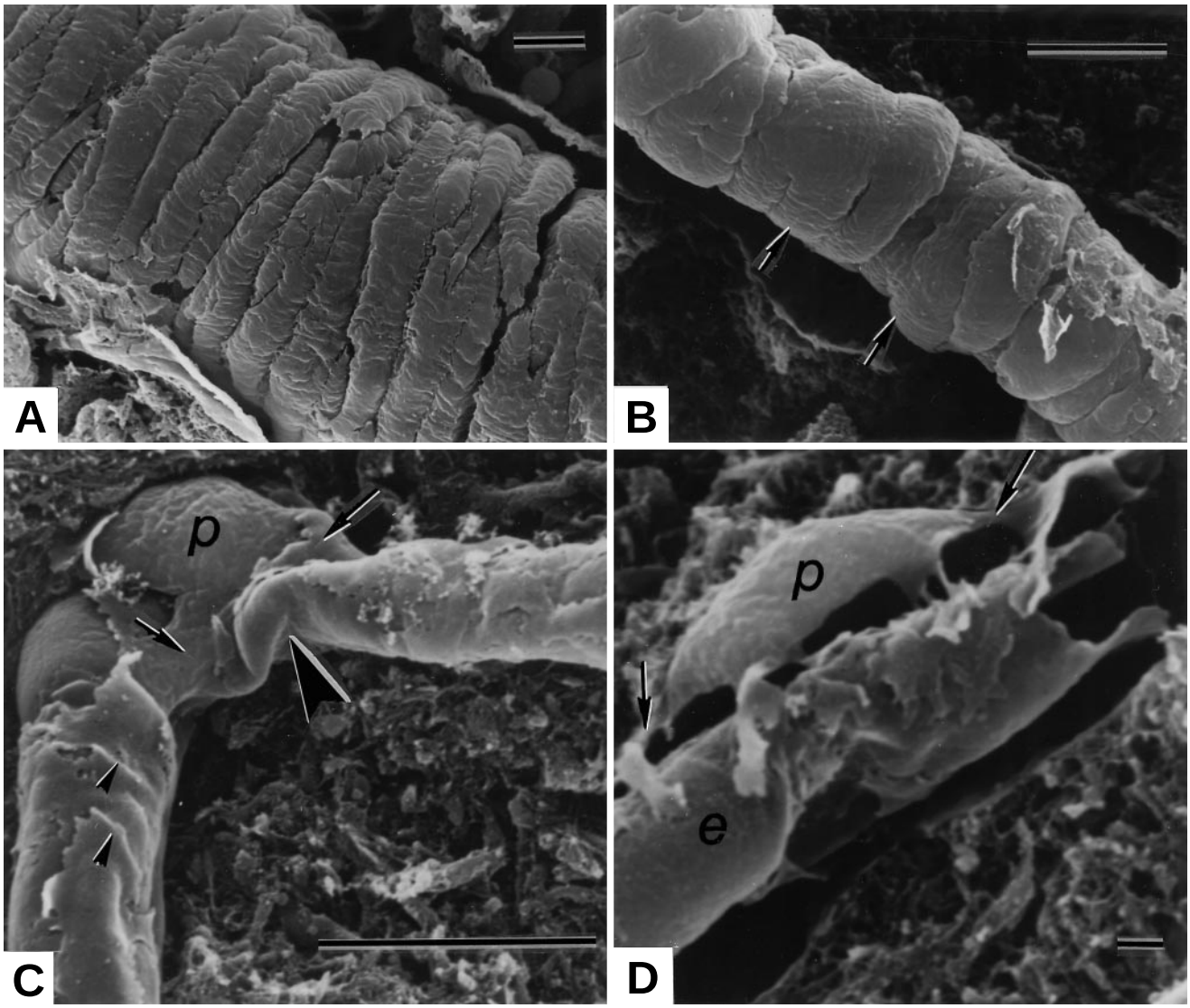

Fig. 6A–D Micrographs at 6 h of reperfusion. **A** A muscular arteriole on the brain surface. Transverse folds remain on the smooth muscle surfaces. **B** A terminal arteriole in the brain parenchyma. Undulations remain on the muscle surfaces. **C** A capillary in the brain parenchyma. The endothelial tube shows tortuousity (*large arrowhead*) near a pericyte cell body (*p*). This cell body has rough contours and extends primary processes (*arrows*) with membrane creases (*arrowheads*). **D** A capillary in the brain parenchyma. A pericyte (*p*) appears nearly detached from the endothelium (*e*). *Arrows* indicate primary processes. *Bars* **A**–**C** = 10 μm, **D** = 1 μm

the brain parenchyma did not differ from that of comparable vessels on the brain surface (Fig. 3D). In contrast, parenchymal precapillary arterioles, measuring 8–10 μm in diameter, had smooth muscle cells of distinct shape. This shape was the result of a bulging cell body with smooth outer surfaces extending broad processes that wound helically around the underlying endothelium (Fig. 3E).The smallest vessel, or intracerebral capillaries, measuring 5–8 μm, had characteristic pericytes throughout their lengths. Pericytes could be differentiated from other cells in that they possesed smooth surfaces and a bulging cell body from which long primary processes extended in an opposite direction to the main axis of the vessel. Primary processes gave rise to numerous smaller secondary processes which were oriented circularly around the vessel. The smooth abluminal surfaces of the endothelium was visible between adjacent pericyte processes which otherwise were closely apposed to the endothelial surfaces (Fig. 3F). No differences in the cytoarchitecture of terminal arterioles, precapillary arterioles, and capillaries were found between control and sham-operated rats.

Experimental (ischemia and reperfusion) animals

Deep transverse or oblique folds were observed on the adventitial surface of all muscular arterioles (Fig. 4A) within seconds after reperfusion. In contrast, shallower folds or undulations were more characteristic on all the terminal arterioles at the same time frame (Fig. 4B). It should be noted that these folds and undulations in experimental brains were found in practically all the smooth

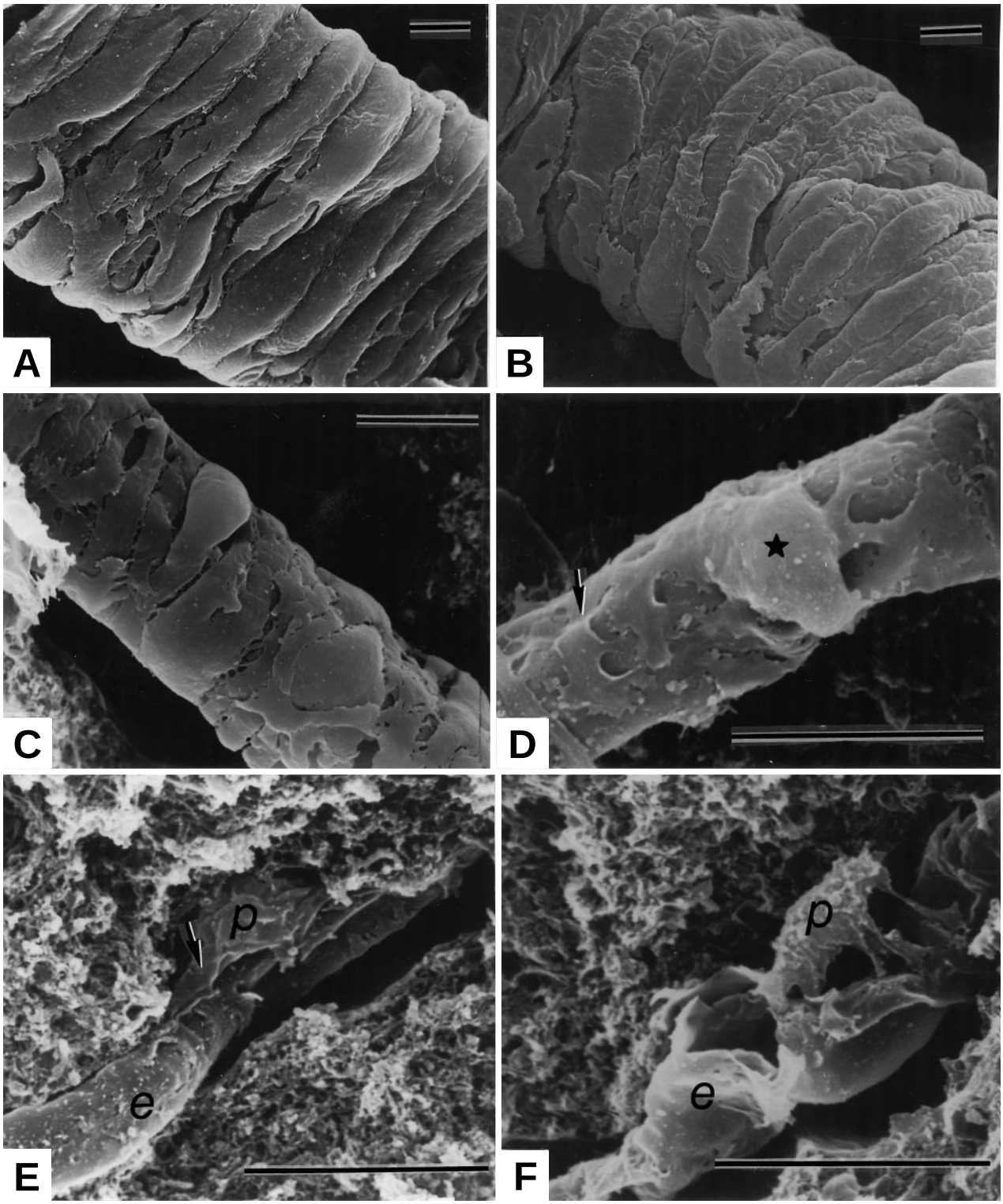

Fig. 7A–F Micrographs at 24 h of reperfusion. **A** A muscular arteriole on the brain surface with muscle cells that have smooth surfaces. **B** Another muscular arteriole on the brain surface. Ripple-like undulations are seen on the smooth muscle surfaces. **C** A terminal arteriole in the brain parenchyma with muscle cells that have smooth surfaces. **D** A precapillary arteriole in the brain parenchyma. A muscle cell of this arteriole has a bulging cell body (*star*) and processes with scalloped contours (*arrow*). **E** A capillary in the brain parenchyma. A pericyte has a cell body (*p*) with rough contours which closely appose the endothelium (*e*). **F** Another pericyte with a cell body (*p*) separated from the endothelium (*e*). This cell body projects several processes to the endothelium in a spider like fashion. *Bars* = 10 μm

muscle cells of single vessels, whereas only few were seen in some cells in controls that were exposed to the same head perfusion pressure. After 8 min of reperfusion, corresponding to the c-CBF maximal hyperemia, folds and undulations completely disappeared and the smooth muscle cells of all arterioles looked distended (Fig. 4C, D). After 15 min of reperfusion, corresponding to the beginning of the c-CBF decline following maximal hyperemia, folds and undulations appeared again in 50% of the observed muscular and terminal arterioles (Fig. 4E, F). During this hyperemic period, there was no obvious change in the shape and arrangement of the smooth muscle cells of precapillary arterioles. Likewise no changes were observed in capillary pericytes.

In the early period of postischemic hypoperfusion (between 30 and 90 min of reperfusion), some folds and undulations remained on the adventitial surface of most (approximately 75%) muscular and terminal arterioles (Fig. 5A, B). In precapillary arterioles, processes of smooth muscle cells became more irregular and acquired scalloped contour (Fig. 5C). In many capillaries, the cell body of pericytes appeared detached from the endothelium, with only the secondary processes maintaining partial apposition with the endothelial wall (Fig. 5D). In spite of these changes the pericyte surface remained smooth. There was no remarkable difference in the cytoarchitecture of the vascular wall of animals with 30-min reperfusion and that of animals with 90-min reperfusion, although c-CBF values became minimal by 90 min of reperfusion.

Folds and undulations were observed on the smooth muscle cell surfaces of most (approximately 75%) muscular and terminal arterioles, respectively, in the late phase of postischemic hypoperfusion (by 6 h of reperfusion; Fig. 6A, B). In addition, the smooth muscle cell processes of precapillary arterioles retained their scalloped contours (not illustrated). Some capillaries appeared severely deformed with the endothelial tubes displaying tortuousity near the cell body of pericytes (Fig. 6C). Other pericytes seemed to be nearly detached from the endothelium (Fig. 6D).

The surfaces of most muscle cells of muscular and terminal arterioles became smooth (Fig. 7A, C) again during the second hyperemia (between 12 and 24 h). However, in a few cases some cells had folds or ripple-like undulations (Fig. 7B). In addition the smooth muscle cell processes of precapillary arterioles were unchanged (Fig. 7D). Two different kinds of pericytes were distinguished on the basis of cell body position. The cell body of some pericytes had irregular surfaces which closely apposed the endothelial tube (Fig. 7E). Other pericyte cell bodies, however, were separated from the endothelial tube by extending several processes to the endothelial tube in a spider-like fashion (Fig. 7F). These morphological changes in pericytes were more pronounced in animals by 24 h of reperfusion.

Discussion

Experimental model

The most widely used rat forebrain ischemia model has been the four arterial vessel occlusion (4VO, paired vertebrals and common carotids) model described by Pulsinelli and Brierley [55]. These investigators reported a poor outcome with patent CBF after occlusion in approximately 25% of their animals, due to reflow via paravertebral muscle branches, as well as the anterior spinal artery [55, 57]. Kameyama et al. [34] developed a three-vessel occlusion (3VO, basilar and common carotids) model whereby distal basilar occlusion eliminated a large portion of the 4VO collateral reflow. However, correlative autoradiographic records of CBF in this 3VO model did not validate completeness of ischemia because of residual flow via anastomoses of the pterygopalatine branch of the internal carotids with more superficial vessels. Shirane et al. [63] extended the 3VO model by developing a 7VO (paired external carotids, and pterygopalatine branches, as well as common carotids and basilar artery) model. In contrast to previous models, their accompanying autoradiograms revealed complete cessation of forebrain CBF. However, this 7VO model was performed under halothane anesthesia and had a high mortality rate due to respiratory complications which developed postoperatively. In the present study, we improved the 7VO model of Shirane et al. by significantly decreasing the postoperative mortality rate. Increased survival was accomplished by carefully reducing the retraction of the trachea and resection of the longus capitis muscle. More importantly, in contrast with previous models, ischemia in our model was accomplished in fully alert, unanesthetized animals. Our physiological results, therefore, were not affected by the potential systemic effects of anesthesia which is known to alter stroke outcome [26, 36, 46]. Taken together, our improvements of the 7VO model increases its reliability for reproducible postischemic injury following ischemia and reperfusion.

c-CBF during ischemia and reperfusion

CBF changes during and after ischemia in the 7VO rat model have been previously examined with radioisotope techniques. Accompanying autoradiograms of whole brain sections have demonstrated a nearly homogeneous CBF in comparatively large regions of the sections [45, 63]. In contrast, the LDF technique normally measures red blood cell flow in microvessels from very small (1 mm^3) volumes of cortical tissue [3]. Measurements of the c-CBF in our study were obtained over the cortical area representing the sensorimotor cortex. This area was then selected to be the center of the tissue sample processed for SEM. Therefore, our c-CBF values were directly correlated with discrete morphological changes of blood vessels belonging to the same cortical region, thus strengthening the correlative nature of the study.

The mean c-CBF fell to less than 20% of the baseline values immediately after inflating the occluders around the common carotid arteries. While this indicated that we did not achieve complete ischemia, the obtained values were below accepted thresholds for the loss of electroencephalogram and evoked potentials [5, 66]. Indication of severe ischemia with low c-CBF in our study was further exemplified by the appearance of a decerebrate posture which was consistently observed in all animals immediately following occlusion. The temporal profile of the c-CBF obtained after occlusion was, therefore, highly reproducible. We found that after 10 min of ischemia there was, initially, a significant reactive hyperemia that lasted approximately 25 min. This was followed by a prolonged postischemic hypoperfusion lasting approximately 8 h. A second, less pronounced hyperemia succeeded the hypoperfusion for the duration of the experiment. Moreover, these perfusional changes occurred without significant changes of the MBP. Our findings suggest that the rheological resistance of cerebral blood vessels may be lower than normal during the hyperemic phases and higher than normal during the hypoperfusion phase. Interestingly, the c-CBF nadir during postischemic hypoperfusion (at 90 min of reperfusion) coincided with a slight MBP decrease, thus suggesting that it could have been reversed by a rise of the MBP.

Lastly, previous CBF temporal profile studies using autoradiographic techniques [38, 56, 60, 67], as well as ^{133}Xe or H_2 clearance techniques [47, 50, 64, 68, 72, 73] did not include many time points or include measurements beyond 6 h after the onset of reperfusion. Therefore, we are first to measure c-CBF changes up to 24 h of reperfusion which allowed us to observe a second hyperemia during this later time frame. What remains unclear from the present study is whether our second hyperemia represents the delayed hyperemia obtained from regions where severe morphological changes have been known to occur after more than 24 h of reperfusion [56].

Cytoarchitecture of vascular smooth muscle

Ushiwata and Ushiki [77] described the normal three-dimensional architecture of smooth muscle in cerebral blood vessels of the rat. Using a method combining KOH-collagenase digestion with SEM, they demonstrated that, while the adventitial surface of muscle cells of arterioles was always smooth, shallow membrane creases or ripple-like undulations were occasionally found in muscular arterioles. Additionally, they did not observed such membrane creases in terminal or precapillary arterioles. Our findings using control and sham-operated animals confirm and extend their observations. While the reason for occasional membrane creases or ripple-like undulations in muscular arteriole is unknown, the preponderant finding of smooth cell membrane in arterioles of all sizes may be correlated with the dilatation of vessels. Such vasodilatation in control animals would be maintained by the sustained pressure delivered during perfusion-fixation for electron microscopy. If this assumption is correct then smooth surfaces devoid of creases on the muscle cell membrane may signal a state of relaxation. Moreover, in our sham-operated rats, we speculate that vasodilatation in the muscular arterioles after vessel occlusion surgery could be a compensatory action in response to a decreased driving force of the CBF which reaches the brain only by way of the internal carotids.

In contrast to the pattern of relaxation in smooth muscle membranes, the appearance of marked surface membrane folds and undulations in experimental brains may be indicative of active vasoconstriction. Such marked creases were never observed in control brains, indicating that tissue fixation by itself did not have a significant effect on smooth muscle contractility. While both folds and undulations are oriented transversely to the long axis of the muscle cells, they differ from each other in that the folds are deeper, more numerous and of uniform waviness than the undulations. Previous investigators [18, 54] have studied structural changes of smooth muscles during contractile states by transmission electron microscopy. According to these studies, constricted muscle cells show indented borders. However, these studies were limited in that the three-dimensional shape of the constricted muscle cell could not be visualized in single ultrathin sections. Recently, several investigators have shown the three-dimensional shape of constricted vascular muscle cells by SEM. Uehara et al. [75] illustrated a presumptive constricted muscular artery with numerous transverse folds in rat brain. MacDonald et al. [42] showed similar folds in smooth muscle of a subarachnoid artery in a monkey subjected to experimental hemorrhage. More recently Takahashi [69] demonstrated folds on the adventitial surface of smooth muscle of an intracranial artery from a patient who died of vasospasm after subarachnoid hemorrhage. Although these studies have provided some correlation of transverse folds with muscular contraction or vasospasm in the larger arteries, no such correlations have ever been made in arterioles in either experimental or pathological conditions. Our correlative study is the first to reveal the presence of folds, undulations and other membrane creases in muscular, terminal and precapillary arterioles. These findings support the notion (as discussed below) that the smooth muscle of these small vessels may play a significant role in the control of the microcirculation through the brain parenchyma during ischemia and reperfusion.

Correlation of crease formation with perfusional alterations during ischemia and reperfusion

This study shows significant correlation between the crease formation in smooth muscle membranes and the measured perfusional alterations during ischemia and reperfusion. These correlations include: (1) marked transverse or oblique membrane folds of smooth muscle cells in arterioles immediately after the ischemic brain was reperfused, (2) smooth surfaces of the muscle cells at the

maximum point of hyperemia, and (3) reappearance of folds and undulations when the c-CBF started to decline. Previous investigators have speculated that the reperfusion hyperemia immediately following ischemia is the result of an onrush of blood through vessels maximally dilated by lactoacidosis and devoid of autoregulation [50, 56, 68]. Our findings do not support the notion that smooth muscle cells are dilated during ischemia. Takagi et al. [68] observed a decreased pial arteriole diameter during global ischemia in cat through an artificially created cranial window. The decreased pial artery diameter was caused by interruption of the blood supply, leading to a loss of intraluminal pressure. Our findings support their observations. Decreased intraluminal pressure might further contribute to a collapse of the wall of arterioles. Does the decreased intraluminal pressure contribute to the fold formation observed immediately after reperfusion? Several investigators have measured c-CBF continuously using LDF in a forebrain ischemia model [16, 17]. They have shown that the transition from reperfusion hyperemia to postischemic hypoperfusion is precipitous, indicating that the decline of c-CBF is caused by vasomotor effects. Our findings support this speculation and further suggest that crease formation both immediately after ischemia and after maximal hyperemia result from acute vasoconstriction. However, the mechanism underlying these effects remains to be elucidated.

Factors other than mechanical ones may also be involved in smooth muscle contractility. Endothelin (ET) [81], one of the most potent endogenous vasoconstrictor substances produced by endothelial cells has attracted attention in the pathogenesis of vasoconstriction [41]. Giuffrida et al. [20] found increased ET immunoreactivity in the brains of Mongolian gerbils subjected to unilateral cerebral ischemia. Barone et al. [2] measured ET levels in rats using microdialysis after 20 min of global ischemia produced by combined common carotid artery occlusion and hypotension. They found that ET levels increased significantly during ischemia, returned to normal levels during early reperfusion (0–30 min), and finally increased again after 30 min. Therefore, ET might be important in regulating the vasoconstriction observed both immediately after reperfusion and when c-CBF declines from the hyperemic plateau. In addition, vasodilating factors other than lactate, such as nitric oxide (NO) produced during and after reperfusion [43] may also contribute to the progression of the hyperperfusion.

Frerichs et al. [17] measured c-CBF using LDF during ischemia and reperfusion after ibotenic acid lesions in rats. They were able to abolish the precipitous decrease of c-CBF from hyperemia to hypoperfusion, suggesting that the rapid c-CBF decrease may be triggered by a local neural mechanism.

In summary, we suggest the following mechanism of reperfusion hyperemia. First, arterioles with dysfunctional autoregulation constrict markedly during ischemia and the initial onrush of blood flow of reperfusion. Second, as the vasoconstrictive factors are metabolized, smooth muscles relax producing vasodilatation and above normal c-CBF. Third, accumulation of vasoconstrictive factors from multiple sources, including adjacent neurons, triggers vasoconstriction and results in a precipitous decline of c-CBF.

As mentioned in the introduction a variety of mechanisms have been proposed to explain the delayed hypoperfusion, including: rheological changes, microvascular obstruction [23, 51] and hemoconcentration; capillary obstruction by endothelial microvilli formation [14]; compression of vascular lumen by cellular and/or extracellular swelling [50, 53], and increased vascular smooth muscle tone [17, 40, 47, 56, 68, 72]. This study supports the last of these explanations, although it does not rule out the others.

Recently, Wisniewski et al. [79] studied cerebral vasospasm of cardiac arrest-related global ischemia in rats by SEM. They illustrated three distinct luminal changes in both veins and arteries. In the present study, we observed similar changes in arterioles and capillaries but could rarely see the abluminal surfaces of veins, because these were destroyed and peeled off when the specimens were punctured and separated prior to SEM analysis.

The present study did not show a clear correlation between the second hyperemia and smooth muscle cell morphology. To explain the second hyperemia two mechanisms have been proposed. Garcia et al. [19] measured CBF and morphometrically analyzed the diameter of capillaries 24 h after transient middle cerebral artery occlusion in monkey. They concluded that postocclusive hyperemia resulted from vasodilatation of capillaries. The other possibility involves the recruitment of previously unperfused microvessels [21], although the concept of recruitment is controversial. Our results show that many muscle cells were smooth during the second hyperemia, thus suggesting arteriolar dilatation. This dilatation could result also from accumulation of vasodilatory substances which can be delivered from damaged cells, such as basic fibroblast growth factor [59], or which are induced after reperfusion, such as NO [8, 43].

Postischemic changes of capillary pericytes

Marked changes in the shape and arrangement of capillary pericytes were observed after ischemia, and were related generally to two types of pericyte conformation: (1) pericytes with cell bodies remaining closely apposed to the endothelium, and (2) pericytes with cell bodies widely separated from the endothelium. Moreover, separation of pericytes coincided with the second period of hyperemia. While the significance of this separation remains unclear, it may signal a possible migration of these cells from the vascular wall into the parenchyma. Pericytes have been reported to migrate into the brain parenchyma under certain conditions [58]. It is thought that, once migrated, the pericyte could become a potential source of microglia [4] and serve as brain macrophage precursors reacting to injury and disease [65]. Our findings support this notion of rapid pericyte migration into the parenchyma preceding the onset of neuronal degeneration which would result

from the ischemic insult. Alternatively, the separation of pericytes from the vascular wall may be a mechanical effect of extravasated plasma [48] from a BBB breakdown after ischemia [9, 37, 60, 67]. In support of this is the observation that, even during this condition, the secondary processes of the pericyte retain their close apposition with segments of the endothelial wall. Furthermore, we noticed that at these points of apposition the wall of the endothelium appears constricted. While active constriction of the endothelium can not be ruled out, such constriction could, conceivably, be effected by the contractile properties of the pericyte processes. Contractile elements such as actin [25], tropomyosin [32], myosin [33], and cyclic GMP-dependent protein kinase [31] have been detected in the pericyte cytoplasm. In addition their contractility has been demonstrated in vitro [35]. Therefore, the present observations together with previous data suggest a role for pericytes in modulating the diameter of the capillary wall, which may contribute to the progression of the postischemic hypoperfusion.

Acknowledgements We thank Sharon Murphy, Chery Owen and Sarah Alousi for their technical assistance. The use of the SEM facility in the Department of Anatomy and Cell Biology is also acknowledged. This work was supported by funds from the Department of Neurosurgery and the Detroit Neurotrauma Institute at Wayne State University.

References

1. Allen K, Busza AL, Crockard HA, Frackowiak RSJ, Gadian DG, Proctor E, Russel RWR, Williams SR (1988) Acute cerebral ischemia: concurrent changes in cerebral blood flow, energy metabolites, pH, and lactate measured with hydrogen clearance and ^{31}P and ^{1}H nuclear magnetic resonance spectroscopy. III. Changes following ischemia. J Cereb Blood Flow Metab 8: 816–821
2. Barone FC, Globus MYT, Price WJ, White RF, Storer BL, Feuerstein GZ, Busto R, Ohlstein EH (1994) Endothelin levels increase in rat focal and global ischemia. J Cereb Blood Metab 14: 337–342
3. Bonner R, Nossal R (1981) Model for laser Doppler measurements of blood flow in tissues. Appl Optics 20: 2097–2107
4. Boya J, Carbonell AL, Calvo J, Borregón A (1987) Ultrastructural study on the origin of rat microglia cells. Acta Anat (Basel) 130: 329–335
5. Branston NM, Symon L, Crockard HA, Pasztor E (1974) Relationship between the cortical evoked potential and local cortical blood flow following acute middle cerebral artery occlusion in the baboon. Exp Neurol 45: 195–208
6. Braunwald E, Kloner RA (1985) Myocardial reperfusion: a double-edged swords? J Clin Invest 76: 1713–1719
7. Charbel FT, Ausman JI, Diaz FG, Malik GM, Dujovny M, Sanders J (1991) Temporary clipping in aneurysm surgery: technique and results. Surg Neurol 36: 83–90
8. Clavier N, Kirsch JR, Hurn PD, Traystman R (1994) Cerebral blood flow is reduced by N′-nitro-L-arginine methyl ester during delayed hypoperfusion in cats. Am J Physiol 267: H174-181
9. Cole DJ, Matsumura JS, Drummond JC, Schultz RL, Wong MH (1991) Time- and pressure-dependent changes in blood-brain barrier permeability after temporary middle cerebral artery occlusion in rats. Acta Neuropathol 82: 266–273
10. Del Zoppo GJ, Zeumer H, Harker LA (1986) Thrombolytic therapy in stroke: possibilities and hazards. Stroke 17: 595–607
11. Dempsey RJ, Roy MW, Meyer K, Cowen DE, Tai HH (1986) Development of cyclooxygenase and lipoxygenase metabolites of arachidonic acid after transient cerebral ischemia. J Neurosurg 64: 118–124
12. Diemer NH, Siemkowicz E (1980) Increased 2-deoxyglucose uptake in hippocampus, globus pallidus and substantia nigra after cerebral ischemia. Acta Neurol Scand 61: 56–63
13. Dietrich WD (1994) Morphological manifestations of reperfusion injury in brain. Ann NY Acad Sci 723: 15–24
14. Dietrich WD, Busto R, Ginsberg MD (1984) Cerebral endothelial microvilli: formation following global forebrain ischemia. J Neuropathol Exp Neurol 43: 72–83
15. Dirnagl U (1993) Cerebral ischemia: the microcirculation as trigger. Prog Brain Res 196: 49-65
16. Dirnagl U, Thorén P, Villringer A, Sixt G, Them A, Eihäupl KM (1993) Global forebrain ischemia in the rat: controlled reduction of cerebral blood flow by hypobaric hypotension and two-vessel occlusion. Neurol Res 15: 128–130
17. Frerichs KU, Sirén AL, Feuerstein GZ, Hallenbeck JM (1992) The onset of postischemic hypoperfusion in rats is precipitous and may be controlled by local neurons. Stroke 23: 399–406
18. Gabella G (1976) Structual changes in smooth muscle cells during isotonic contraction. Cell Tissue Res 170: 187–201
19. Garcia JH, Lowry SL, Briggs L, Mitchem HL, Morawetz R, Halsey JH, Conger KA (1983) Brain capillaries expand and rupture in areas of ischemia and reperfusion. In: Reivich M, Hurtig HI (eds) Cerebrovascular diseases. Raven Press, New York, pp 169-182
20. Giuffrida R, Bellomo M, Polizzi G, Malatino LS (1992) Ischemia-induced changes in the immunoreactivity for endothelin and other vasoactive peptides in the brain of the mongolian gerbil. J Cardiovas Pharmacol 20 [Suppl 12]: S41–S44
21. Gjedde A, Kuwabara H, Hakim AM (1990) Reduction of functional capillary density in human brain after stroke. J Cereb Blood Flow Metab 10: 317–326
22. Hallenbeck JM, Dutka AJ (1990) Background review and current concepts of reperfusion injury. Arch Neurol 47: 1245–1254
23. Hallenbeck JM, Dutka AJ, Tanishima T, Kochanek PM, Kumaroo KK, Thompson CB, Obrenovitch TP, Contreras TJ (1986) Polymorphonuclear leukocyte accumulation in brain regions with low blood flow during the early postischemic period. Stroke 17: 246–253
24. Hamann GF, Del Zoppo GJ (1994) Leukocyte involvement in vasomotor reactivity of the cerebral vasculature. Stroke 25: 2117–2119
25. Herman IM, D'amore PA (1985) Microvascular pericytes contain muscle and nonmuscle actins. J Cell Biol 101: 43–52
26. Hoffman WE, Thomas C, Albrecht RF (1993) The effect of halothane and isoflurane on neurologic outcome following incomplete ischemia in the rat. Anesth Analg 76: 279–283
27. Hossmann KA, Sasaki S, Kimoto K (1976) Cerebral uptake of glucose and oxygen in the cat brain after prolonged ischemia. Stroke 7: 301–305
28. Ikeda Y, Long DM (1990) The molecular basis of brain injury and brain edema: the role of oxygen free radicals. Neurosurgery 27: 1–11
29. Jabre A, Symon L (1987) Temporary vascular occlusion during aneurysm surgery. Surg Neurol 27: 47–63
30. Johansson BB, Nordborg C, Westergren I (1990) Neuronal injury after a transient opening of the blood-brain barrier: modifying factors. In: Johansson BB, Owman C, Widner H (eds) Pathophysiology of the blood-brain barrier. Elsvier, Amsterdam, pp 145-157
31. Joyce NC, DeCamilli P, Boyles J (1984) Pericytes, like vascular smooth muscle cells, are immunocytochemically positive for cyclic GMP-dependent protein kinase. Microvasc Res 28: 206–219
32. Joyce NC, Haire MF, Palade G (1985) Contractile proteins in pericytes. I. Immunoperoxidase localization of tropomyosin. J Cell Biol 100: 1379–1386

33. Joyce NC, Haire MF, Palade G (1985) Contractile proteins in pericytes. II. Immunocytochemical evidence for the presence of two isomyosins in graded concentrations. J Cell Biol 100: 1387–1395
34. Kameyama M, Suzuki J, Shirane R, Ogawa A (1985) A new model of bilateral hemispheric ischemia in the rat-three vessel occlusion model. Stroke 16: 489–493
35. Kelley C, D'Amore P, Hechtman HB, Shepro D (1987) Microvascular pericyte contractility in vitro: comparison with other cells of the vascular wall. J Cell Biol 104: 483–490
36. Kofke WA, Nemoto EM, Hossmann KA, Taylor F, Kessler PD, Stezoski W (1979) Brain blood flow and metabolism after global ischemia and post-insult thiopental therapy in monkeys. Stroke 10: 554–560
37. Kuroiwa T, Ting P, Martinez H, Klatzo I (1985) The biphasic opening of the blood-brain barrier to proteins following temporary middle cerebral artery occlusion. Acta Neuropathol (Berl) 68: 122–129
38. Levy DE, Van Uitert RL, Pike CL (1979) Delayed postischemic hypoperfusion: a potentially damaging consequence of stroke. Neurology 29: 1245–1253
39. Loftus CM, Quest DO (1995) Technical issues in carotid artery surgery. Neurosurgery 36: 629–647
40. Louis TM, Meng W, Bari F, Errico RA, Busija DW (1996) Ischemia reduces CGRP-induced cerebral vascular dilatation in piglets. Stroke 27: 134–139
41. Lüscher TF (1993) Do we need endothelin antagonists? Cardiovas Res 27: 2089–2093
42. MacDonald RL, Weir BKA, Chen MH, Grace MGA (1991) Scanning electron microscopy of normal and vasospastic monkey cerebrovascular smooth muscle cells. Neurosurgery 29: 544–550
43. Malinski T, Bailey F, Zhang ZG, Chopp M (1993) Nitric oxide measured by a porphyrinic microsensor in rat brain after transient middle cerebral artery occlusion. J Cereb Blood Flow Metab 13: 355–358
44. Mchedlishvili GI, Baramidze DG, Nikolaishvili LS, Antia RV, Gordeladze ZT (1978) On the control of microcirculation in the cerebral cortex during and following ischemia. Biochem Exp Biol 14: 285–297
45. Melgar MA, Diaz FG, Rafols JA (1995) Ultrastructual changes in the blood brain barrier after global forebrain ischemia-reperfusion in an unanesthetized rat model. Abstracts of the 63rd American Association of Neurological Surgeons Annual Meeting. AANS, Orlando, Fl, April 1995, p 4
46. Michenfelder JD (1974) The interdependency of cerebral functional and metabolic effects following massive doses of thiopental in the dog. Anesthesiology 41: 231–236
47. Miller CL, Lampard DG, Alexander K, Brown WA (1980) Local cerebral blood flow following transient cerebral ischemia. I. Onset of impaired reperfusion within the first hour following global ischemia. Stroke 11: 534–541
48. Miller FN, Sims DE, Schuschke DA, Abney DL (1992) Differentiation of light-dye effects in the microcirculation. Microvasc Res 44: 166–184
49. Murakami T (1973) A metal impregnation method of biological specimens for scanning electron microscopy. Arch Histol Jpn 35: 323–326
50. Nemoto EM, Snyder JV, Carroll RG, Morita H (1975) Global ischemia in dogs: cerebrovascular CO_2 reactivity and autoregulation. Stroke 6: 425–431
51. Obrenovitch TP, Hallenbeck JM (1985) Platelet accumulation in regions of low blood flow during the postischemic period. Stroke 16: 224–234
52. Paxinos G, Watson C (1986) The rat brain in stereotaxic coordinates, 2nd edn. Academic Press, New York
53. Petito CK, Pulsinelli WA, Jacobson G, Plum F (1982) Edema and vascular permeability in cerebral ischemia: comparison between ischemic neuronal damage and infarction. J Neuropathol Exp Neurol 41: 423–436
54. Phelps PC, Luft JH (1969) Electron microscopical study of relaxation and constriction in frog arterioles. Am J Anat 125: 399–428
55. Pulsinelli WA, Brierley JB (1979) A new model of bilateral hemispheric ischemia in the unanesthetized rat. Stroke 3: 267–272
56. Pulsinelli WA, Levy DE, Duffy TE (1982) Regional cerebral blood flow and glucose metabolism following transient forebrain ischemia. Ann Neurol 11: 499–509
57. Pulsinelli WA, Levy DE, Duffy TE (1983) Cerebral blood flow in the four-vessel occlusion rat model (letter). Stroke 14: 832–833
58. Rafols JA, Owen C, Murphy S, Dore-Duffy P (1995) Pericyte response following traumatic brain injury: migration of pericytes from CNS microvessels and apoptosis. J Neurotrauma 12: 988
59. Rosenblatt S, Irikura K, Caday CG, Finklestein SP, Moskowitz MA (1994) Basic fibroblast growth factor dilates rat pial arterioles. J Cereb Blood Flow Metab 14: 70–74
60. Sage JI, Van Uitert RL, Duffy TE (1984) Early changes in blood-brain barrier permeability to small molecules after transient cerebral ischemia. Stroke 15: 46–50
61. Sato A, Uchida S, Yamauchi Y (1994) A new method for continuous measurement of regional cerebral blood flow using laser Doppler flowmetry in a conscious rat. Neurosci Lett 175: 149–152
62. Shiraishi T, Sakaki S, Uehara Y (1986) Architecture of the media of the arterial vessels in the dog brain: a scanning electron-microscopic study. Cell Tissue Res 243: 329–335
63. Shirane R, Shimizu H, Kameyama M, Weinstein P (1991) A new method for producing temporary complete cerebral ischemia in rats. J Cereb Blood Flow Metab 11: 949–956
64. Snyder JV, Nemoto EM, Carroll RG, Safar P (1975) Global ischemia in dogs: intracranial pressures, brain blood flow and metabolism. Stroke 6: 21–27
65. Streit WJ, Kreutzberg GW (1988) Response of endogenous glial cells to motor neuron degeneration induced by toxin ricin. J Comp Neurol 268: 248–263
66. Sundt TM, Sharbrough FW, Anderson RE, Michenfelder JD (1974) Cerebral blood flow measurements and electroencephalograms during carotid endarterectomy. J Neurosurg 41: 310–320
67. Suzuki R, Yamaguchi T, Kirino T, Orzi F, Klatzo I (1983) The effects of 5-minute ischemia in mongolian gerbils. I. Blood-brain barrier, cerebral blood flow, and local cerebral glucose utilization changes. Acta Neuropathol (Berl) 60: 207–216
68. Takagi S, Cocito L, Hossmann KA (1977) Blood recirculation and pharmacological responsiveness of the cerebral vasculature following prolonged ischemia of cat brain. Stroke 8: 707–712
69. Takahashi A (1994) A scanning electron microscopic study on the smooth muscle cells of human intracranial arteries. – Normal and pathological. Hokkaido Igaku Zasshi 69: 1455–1467
70. Takahashi A, Ushiki T, Abe K, Houkin K, Abe H (1994) Cytoarchitecture of periendothelial cells in human cerebral venous vessels as compared with the scalp vein. A scanning electron microscopic study. Arch Histol Cytol 57: 331–339
71. Takahashi A, Ushiki T, Abe K, Houkin K, Abe H (1994) Scanning electron microscopic studies of the medial smooth muscles in human major intracranial arteries. Arch Histol Cytol 57: 341–350
72. Todd NV, Picozzi P, Crockard HA, Russell RR (1986) Reperfusion after cerebral ischemia: influence of duration of ischemia. Stroke 17: 460–466
73. Traupe H, Kruse E, Heiss WD (1982) Reperfusion of focal ischemia of varying duration: postischemic hyper- and hypoperfusion. Stroke 13: 615–622
74. Traystman RJ, Kirsch JR, Koehler RC (1991) Oxygen radical mechanisms of brain injury following ischemia and reperfusion. J Appl Physiol 71: 1185–1195

75. Uehara Y, Fujiwara T, Kaido T (1990) Morphology of vascular smooth muscle fibers and pericytes: scanning electron microscopic studies. In: Motta PM (ed) Ultrastructure of smooth muscle cell. Kluwer, Boston, pp237-251
76. Ushiki T, Ide C (1988) A modified KOH-collagenase method applied to scanning electron microscopic observations of peripheral nerves. Arch Histol Cytol 51: 223–232
77. Ushiwata I, Ushiki T (1990) Cytoarchitecture of the smooth muscles and pericytes of rat cerebral blood vessels. J Neurosurg 73: 82–90
78. White BC, Grossman LI, Krause GS (1993) Brain injury by global ischemia and reperfusion: a theoretical perspective on membrane damage and repair. Neurology 43: 1656–1665
79. Wisniewski HM, Pluta R, Lossinsky AS, Mossakowski MJ (1995) Ultrastructural studies of cerebral vascular spasm after cardiac arrest-related global cerebral ischemia in rats. Acta Neuropathol 90: 432–440
80. Yamaguchi T, Hayakawa T, Kikuchi H (1993) Intravenous tissue plasminogen activator in acute thromboembolic stroke: a placebo controlled, double blind trial. In: Del Zoppo GJ, Mori E, Hacke W (eds) Thrombolytic theray in acute ischemic stroke, vol 2. Springer, Berlin Heidelberg New York, pp 59-65
81. Yanagisawa M, Kurihara H, Kimura S, Tomobe Y, Kobayashi M, Mitsui H, Yazaki Y, Goto K, Masaki T (1988) A novel potent vasoconstrictor peptide produced by vascular endothelial cells. Nature 332: 411–415